Environmental Science & Technology

Article

pubs.acs.org/est

Sulfidization of Organic Freshwater Flocs from a Minerotrophic Peatland: Speciation Changes of Iron, Sulfur, and Arsenic

Laurel K. ThomasArrigo,[†] Christian Mikutta,*[,†,‡] Regina Lohmayer,[§] Britta Planer-Friedrich,[§] and Ruben Kretzschmar[†]

[†]Soil Chemistry Group, Institute of Biogeochemistry and Pollutant Dynamics, ETH Zurich, 8092 Zurich, Switzerland

[‡]Section for Environmental Chemistry and Physics, Department of Plant and Environmental Sciences, University of Copenhagen, DK-1871 Frederiksberg C, Denmark

[§]Department of Environmental Geochemistry, Bayreuth Center for Ecology and Environmental Research (BAYCEER), Bayreuth University, 95440 Bayreuth, Germany

Supporting Information

ABSTRACT: Iron-rich organic flocs are frequently observed in surface waters of wetlands and show a high affinity for trace metal(loid)s. Under low-flow stream conditions, flocs may settle, become buried, and eventually be subjected to reducing conditions facilitating trace metal(loid) release. In this study, we reacted freshwater flocs (704−1280 mg As/kg) from a minerotrophic peatland (*Gola di Lago*, Switzerland) with sulfide (5.2 mM, $S(-II)_{spike}$/Fe = 0.75−1.62 mol/mol) at neutral pH and studied the speciation changes of Fe, S, and As at 25 ± 1 °C over 1 week through a combination of synchrotron X-ray techniques and wet-chemical analyses. Sulfidization of floc ferrihydrite and nanocrystalline lepidocrocite caused the rapid formation of mackinawite (52−81% of Fe_{solid} at day 7) as well as solid-phase associated S(0) and polysulfides. Ferrihydrite was preferentially reduced over lepidocrocite, although neoformation of lepidocrocite from ferrihydrite could not be excluded. Sulfide-reacted flocs contained primarily arsenate (47−72%) which preferentially adsorbed to Fe(III)-(oxyhydr)oxides, despite abundant mackinawite precipitation. At higher $S(-II)_{spike}$/Fe molar ratios (≥1.0), the formation of an orpiment-like phase accounted for up to 35% of solid-phase As. Despite Fe and As sulfide precipitation and the presence of residual Fe(III)-(oxyhydr)oxides, mobilization of As was recorded in all samples (As_{aq} = 0.45−7.0 μM at 7 days). Aqueous As speciation analyses documented the formation of thioarsenates contributing up to 33% of As_{aq}. Our findings show that freshwater flocs from the *Gola di Lago* peatland may become a source of As under sulfate-reducing conditions and emphasize the pivotal role Fe-rich organic freshwater flocs play in trace metal(loid) cycling in S-rich wetlands characterized by oscillating redox conditions.

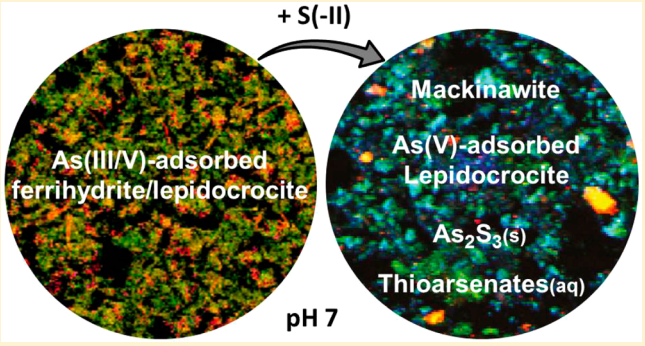

INTRODUCTION

Organic flocs—complex associations of microorganisms, their exudates, mineral phases, and organic detritus—are commonly identified in freshwater wetlands and tend to show high affinities for trace metal(loid)s.[1−3] Flocs are in constant interaction with their aqueous geochemical surroundings[4] and as such are exposed to short-term events (storm and flooding) which can alter the prevailing water flow conditions and thus floc mobility and composition.[5−7] For example, Plach et al.[2] reported significant concentration increases of Ag (from 0.01 to 7.35 μmol/g) and Cu (from 0.60 to 1.45 μmol/g) in flocs following storm events, as well as surges in crystalline Fe/Mn-(oxyhydr)oxide-associated metal(loid)s in storm-sampled flocs, likely due to mineral phase contributions from mobilized bed sediments. Seasonal changes in geochemical conditions may also affect the microbial and mineralogical composition of flocs. Elliot et al.[8] followed seasonal changes in floc microbial communities and noted their corresponding effect on Fe mineralogy and floc Cd and Pb content. They found a temperature- and light-driven shift between "summer" flocs, which contained Fe-metabolizing bacteria and primarily amorphous FeOOH mineral phases, and "winter" flocs characterized by a relative enrichment in iron- and sulfate-reducing bacteria and organic/sulfide associated Fe(II). In agreement with the seasonal changes in microbial floc communities, "summer" flocs showed elevated Cd and Pb contents (~0.01 and ~0.50 μmol/g, respectively), whereas "winter" floc Cd and Pb contents were an order of magnitude lower.[8] Despite these important insights into the coupling

Received: November 24, 2015
Revised: February 12, 2016
Accepted: February 25, 2016
Published: March 11, 2016

DOI: 10.1021/acs.est.5b05791
Environ. Sci. Technol. 2016, 50, 3607−3616

between microbial community composition and Fe mineralogy in flocs, mineralogical changes in flocs subject to reducing conditions are still poorly understood. Particularly the linkage between microbial sulfidogenesis and concomitant speciation changes of floc-associated trace metal(loid)s remains elusive, information which is critical to understanding trace metal(loid) cycling in freshwater wetlands.

In a previous study,[3] we have investigated the speciation of Fe and As in organic flocs from streambeds (pH 5.3−6.3) of the As-enriched minerotrophic peatland *Gola di Lago*, Switzerland,[9,10] using ^{57}Fe Mössbauer spectroscopy and synchrotron X-ray techniques. The flocs contained up to 22 wt % Fe and 2620 mg/kg As (arsenite and arsenate) bound in monodentate-binuclear ("bridging") surface complexes to ferrihydrite (e.g., ~$Fe_5HO_8{\cdot}4H_2O$) and disordered, X-ray amorphous lepidocrocite (γ-FeOOH). Additionally, we found evidence for extensive bioaccumulation of As in floc-associated green algae (*Closterium* spp.).[3] *Gola di Lago* flocs tend to settle under low-flow conditions,[3] and through burial and/or seasonally induced shifts in the dominant microbial groups may eventually be subjected to sulfate-reducing conditions, facilitating changes in floc mineralogy[8] and, potentially, the mobilization of floc-associated As. Ferrihydrite and lepidocrocite both readily oxidize sulfide, and the small crystallite size of floc lepidocrocite may further encourage sulfidization by increasing the availability of reactive surface sites.[3,11,12] Sulfidization reactions are highly pH dependent, and involve a rapid electron transfer between Fe(III) and surface-complexed sulfide which results in elemental S (S(0)) and surface-associated Fe(II):[11]

$$2Fe(OH)_3 + H_2S + 4H^+ \leftrightarrow 2Fe^{2+} + S(0) + 6H_2O \quad (1)$$

$$2FeOOH + H_2S + 4H^+ \leftrightarrow 2Fe^{2+} + S(0) + 4H_2O \quad (2)$$

Dissolution of Fe(II) leads to $Fe(II)_{aq}$, which can interact with excess sulfide, precipitating nanocrystalline mackinawite (tetragonal FeS):[11]

$$Fe^{2+} + HS^- \leftrightarrow FeS_{(s)} + H^+ \quad (3)$$

Alternatively, excess Fe(II) can interact with existing Fe(III)-(oxyhydr)oxides to form magnetite (Fe_3O_4)[13−15] or green-rusts ($[Fe(II)_{1-n}Fe(III)_n(OH)_2]^{n+}(CO_3,Cl,SO_4)^{n-}$),[15] facilitate the mineralogical transformation of ferrihydrite into lepidocrocite or goethite (α-FeOOH),[14,16] or promote the recrystallization of Fe(III)-(oxyhydr)oxides.[16]

Microbial reduction of As-bearing Fe(III)-(oxyhydr)oxides is known to enhance the mobility of As,[15,17−20] though released As may partially be immobilized by residual Fe(III)-(oxyhydr)-oxides,[15,21] or secondary mineral phases such as Fe sulfides (mackinawite and pyrite (FeS_2))[21] or mixed-valence Fe minerals.[22] Farquhar et al.[21] showed that mackinawite − the initial mineral product of Fe(III)-(oxyhydr)oxide sulfidization − has a high sorption capacity for As at pH 5.5−6.5, taking up 80−93% of initial As_{aq} (0.04−0.20 mM) provided as arsenite or arsenate. Yet, As mobilized through reaction of sulfide with floc ferrihydrite or lepidocrocite may preferentially sorb to residual Fe(III) minerals.[15] Alternatively, mobilized arsenite may react with S(0) and sulfide to form (oxy)thioarsenates ($AsO_xS_{4-x}^{3-}$, x = 0−3),[23−25] aqueous arsenate species with a lower affinity toward mackinawite and crystalline Fe(III)-oxyhydroxides (e.g., goethite) than arsenate or arsenite.[26,27] In sulfidic solutions, As may also precipitate as As sulfide minerals such as orpiment (As_2S_3) or realgar (α-As_4S_4),[28] as reported for shallow peat layers of the *Gola di Lago* peatland.[10,29] Moreover, the reaction of sulfide with floc organic matter (OM) may result in the formation of arsenite-sequestering sulfhydryl groups,[30] though this may be limited by the low aromaticity of floc OM.[3] The net effect of floc sulfidization on the mobilization and speciation of floc-associated As, however, remains unknown. To study this, we reacted *Gola di Lago* freshwater flocs with sulfide at neutral pH and studied the speciation changes of Fe, S, and As through a combination of synchrotron X-ray techniques and wet-chemical analyses. Specifically, we tested the hypothesis that sulfidization of As-containing flocs leads to a net mobilization of As, rendering *Gola di Lago* flocs an important source for As under reducing conditions.

MATERIALS AND METHODS

Floc Sampling, Preparation, and Characterization. Floc material was collected from streambeds of sites 5 and 6 of the *Gola di Lago* peatland (Figure S1) in October 2013. The flocs were collected in beakers, allowed to settle overnight, and then decanted, transported to the laboratory, and stored at 4 °C in darkness until further processing. In order to obtain information on the size-dependent reactivity of flocs, the flocs were separated into <40 μm and 40−250 μm size fractions, hereafter referred to as, for example, '5S' and '5L' (small and large flocs from site 5, respectively). To obtain floc size fractions, coarse wet floc material (0.3 L) was suspended in 0.5 L of deionized water, shaken overhead for 20 min (50 rpm), and ultrasonicated (1440 J/g, 40 min) in an ice bath. Dispersed floc material was then wet-sieved with deionized water (~1.8 L/min; Retsch sieving machine). Fractionated flocs were repetitively washed with doubly deionized (DI) water (18.2 MΩ cm), centrifuged, then flash-frozen with liquid N_2, freeze-dried, manually homogenized, and stored in brown-glass bottles in a desiccator. At the time of floc collection, surrounding surface waters were also analyzed on-site for standard geochemical parameters and for aqueous element concentrations as described in ref 3 (Table S1). Total element contents of the flocs were determined after microwave-assisted acid digestion (MLS turboWave) using inductively coupled plasma-optical emission spectrometry (ICP-OES, Vista-MPX, Varian), and total C and N contents were analyzed with an elemental analyzer (CHNS-932, LECO). Qualitative mineral phase analyses were performed by X-ray diffraction (XRD, D8 Advance, Bruker). Homogenized floc samples were anoxically loaded into 1 mm o.d. borosilicate glass capillaries and analyzed in Bragg−Brentano geometry using Cu Kα radiation (λ = 1.5418 Å, 40 kV and 40 mA) and a high-resolution energy-dispersive 1-D detector (LYNXEYE). Diffractograms were recorded from 10 to 80°2θ with a step size of 0.02°2θ and 10 s acquisition time per step.

Sulfidization Experiment. The experiment was conducted in triplicates in an anoxic glovebox (<10 ppm (v/v) O_2). All solutions used were prepared from anoxic DI water. Ca. 0.25 g of floc material was weighed into serum bottles and equilibrated for 16 h in 230 mL of 10 mM 3-(*N*-morpholino)-propanesulfonic acid (MOPS) buffer adjusted to pH 7. Aliquots (20 mL) of a freshly prepared sulfide stock solution (65 mM $Na_2S{\cdot}9H_2O$ in 10 mM MOPS, pH 7) were added to the serum bottles, which were then capped with butyl rubber stoppers. The final sulfide concentration in each serum bottle was 5.2 mM, representative of the maximum sulfide concentration seen in porewater profiles from natural wetlands.[31−35] The resulting $S(-II)_{spike}$/Fe molar ratios ranged from 0.75 to 1.62

DOI: 10.1021/acs.est.5b05791
Environ. Sci. Technol. 2016, 50, 3607−3616

(Table S7), thus partially exceeding the S(-II)/Fe molar ratio of 1.5 required for the stoichiometric reduction of all Fe(III) to $FeS_{(s)}$ according to eqs 1−3.[11]

All serum bottles were wrapped in Al foil and horizontally shaken (150 rpm) at 25 ± 1 °C for 1 week. The pH was maintained at 7.0 ± 0.1 throughout the experiment, and the redox potential (E_h) was monitored regularly. Sulfide-free controls were included for each sample to quantify aqueous As and Fe releases stemming from floc dissolution. Sulfide losses due to volatilization and sampling were found to be negligible (Figure S2). Aliquots for aqueous-phase analysis (14 mL) were taken at 0, 0.3, 3, and 7 days, and 85 mL aliquots were taken at 0.3 and 7 days for solid-phase analysis. Sulfide spiked serum bottles and unreacted floc samples for solid-phase analysis at t = 0 days were prepared concurrently in separate serum bottles. Floc material for solid-phase analysis was collected on 0.45-μm cellulose filters and thoroughly rinsed with DI water. The filter residues were covered and dried in the glovebox atmosphere (N_2). Triplicate samples were combined, homogenized with a mortar and pestle, and stored in darkness until further analyses. Total element contents and XRD measurements of the reacted flocs were determined as described above. Solution samples were passed through 0.22-μm nylon filters and analyzed for dissolved As and Fe by inductively coupled plasma-mass spectrometry (ICP-MS, 7500ce, Agilent).

Aqueous Arsenic Speciation. Arsenite, arsenate, and thioarsenate species were determined in 0.22-μm filtrates by coupled ion chromatography (IC, Dionex ICS-3000; AG/AS16 IonPac column, 20−100 mM NaOH at a flow rate of 1.2 mL/min) and ICP-MS (Thermo-Fisher XSeries2; equipped with a dynamic reaction cell to measure As and S in oxygen mode as AsO^+ (m/z 91) and SO^+ (m/z 48)).[36] Calibration standards were prepared from sodium arsenate dibasic-heptahydrate ($Na_2HAsO_4{\cdot}7H_2O$, Fluka) and sodium (meta)arsenite ($NaAsO_2$, Fluka). Due to a lack of commercial standards, thioarsenates were quantified via the arsenate calibration curve. The validity of this approach has been shown previously.[36]

Aqueous Sulfur Speciation. Thiosulfate ($S_2O_3^{2-}$) and sulfate were determined by IC-ICP-MS in the same run as the As and As−S species described above. Calibration standards were sodium thiosulfate ($Na_2S_2O_3$, Sigma-Aldrich) and ammonium sulfate ($(NH_4)_2SO_4$, Fluka). Dissolved sulfide (H_2S, HS^-, S^{2-}, and colloidal FeS) in 0.22-μm filtrates was quantified with the methylene blue method[37] using a Cary 50 UV−vis spectrophotometer and a detection wavelength of 665 nm. Polysulfide analysis was performed according to the method published by Kamyshny et al.,[38] which is based on the derivatization of labile inorganic polysulfides to form more stable dimethylpolysulfanes. Both 0.22-μm filtered and unfiltered samples were derivatized in this study. For the filtered samples, 200 μL of a sample solution was added simultaneously with 10 μL of methyl trifluoromethanesulfonate ($CF_3SO_3CH_3$, Sigma-Aldrich) to 800 μL of methanol (H_3COH, VWR). For the unfiltered samples, 400 μL of a sample suspension was added simultaneously with 15 μL of methyl trifluoromethanesulfonate to 1600 μL of methanol. After derivatization these solutions were also filtered. All samples were stored frozen until analysis. Dimethylpolysulfanes were analyzed by high performance liquid chromatography (HPLC, Merck Hitachi, L-2130 pump, L-2200 autosampler, L-2420 UV−vis detector) using a reversed phase C18 column (Waters-Spherisorb, ODS2, 5 μm, 250 × 4.6 mm) and a methanol−water gradient elution at 1 mL/min for separation.[39] The injection volume was 100 μL, and the detection wavelength was 230 nm. For quantification, commercially available standards (methyl disulfide, $C_2H_6S_2$, Acros Organics; dimethyl trisulfide, $C_2H_6S_3$, Acros Organics) and fractions of synthesized dimethylpolysulfane reference material[39] were used. Determination of S(0) followed a modified method published by Kamyshny et al.[40] Initially, sulfide was precipitated by adding 25 μL of 200 g/L Zn acetate ($Zn(CH_3COO)_2{\cdot}2H_2O$, Merck) to 725 μL of an (un)filtered sample. Zinc acetate also reacts with the sulfide group of polysulfides, leading to the conversion of zerovalent S in polysulfides to S(0) and consequently the codetermination of polysulfide-bound zerovalent S. The fixed samples were stored frozen until further processing. The extraction of S(0) was performed by addition of 600 μL of chloroform ($CHCl_3$, VWR) and shaking for 1 h. Chloroform extracts were analyzed by HPLC using a reversed phase C18 column (Phenomenex, Luna, 3 μm, 150 × 2.0 mm), and elution was performed with 100% methanol (H_3COH, VWR) at a flow rate of 0.2 mL/min. The injection volume was 5 μL, and the detection wavelength was 254 nm. Calibration standards were prepared by dissolving elemental S powder (reagent grade, purified by sublimation, up to 100-mesh particle size, Sigma-Aldrich) in chloroform.

Synchrotron Measurements. To determine speciation changes of solid-phase Fe, S, and As in flocs after reaction with sulfide, (un)reacted flocs were analyzed by bulk Fe K-edge (7112 eV), S K-edge (2472 eV), and As K-edge (11867 eV) X-ray absorption spectroscopy (XAS) at beamlines 4-1, 4-3, and 11-2 (respectively) of the Stanford Synchrotron Radiation Lightsource (SSRL, Menlo Park, CA, USA). The measurements were performed in fluorescence (Fe, S, and As) and transmission (Fe) mode at cryogenic temperatures. In order to obtain information on the distribution of Fe and As and their local speciation in (un)reacted flocs, selected floc samples were analyzed at room temperature by microfocused X-ray fluorescence (μ-XRF) spectrometry and microfocused X-ray absorption spectroscopy (μ-XAS) at beamline 13 ID-E of the Advanced Photon Source (APS, Chicago, Il, USA). For these analyses, floc material was resuspended in DI water and dried on As-free glass slides (AF37, Päzisions Glas & Optik GmbH). All samples were prepared, stored, and transported anoxically. The bulk XAS samples remained anoxic until the end of analyses. Potential sample oxidation during μ-XRF and μ-XAS measurements was minimized by a constant He stream. Details on all measurements, data reduction, and analyses are provided in the Supporting Information (SI).

RESULTS AND DISCUSSION

Initial Floc Characterization. Floc As contents were higher in samples 5S and 5L (1280 and 1230 mg/kg As, respectively) than in samples 6S and 6L (704 and 707 mg/kg As, respectively), and floc Fe and C contents ranged from 18 to 39 and 18 to 29 wt %, respectively (Table S6). Initial floc Fe/As and Fe/C molar ratios varied between 339−552 and 0.13−0.45, respectively, and all floc samples contained between 5.20 and 7.92 g/kg S.

Solution Trends in Sulfide, Iron, and Redox Potential. All samples showed rapid depletion of dissolved sulfide within the first 20 min, with no detectable sulfide after 160 min (Figure S2). These trends likely result from the quick and complete oxidation of sulfide by floc Fe(III)-(oxyhydr)oxides,[13] though underestimation of dissolved sulfide by the methylene blue method caused by thiosulfate[37,41] or organic thiol[41]

DOI: 10.1021/acs.est.5b05791
Environ. Sci. Technol. 2016, 50, 3607−3616

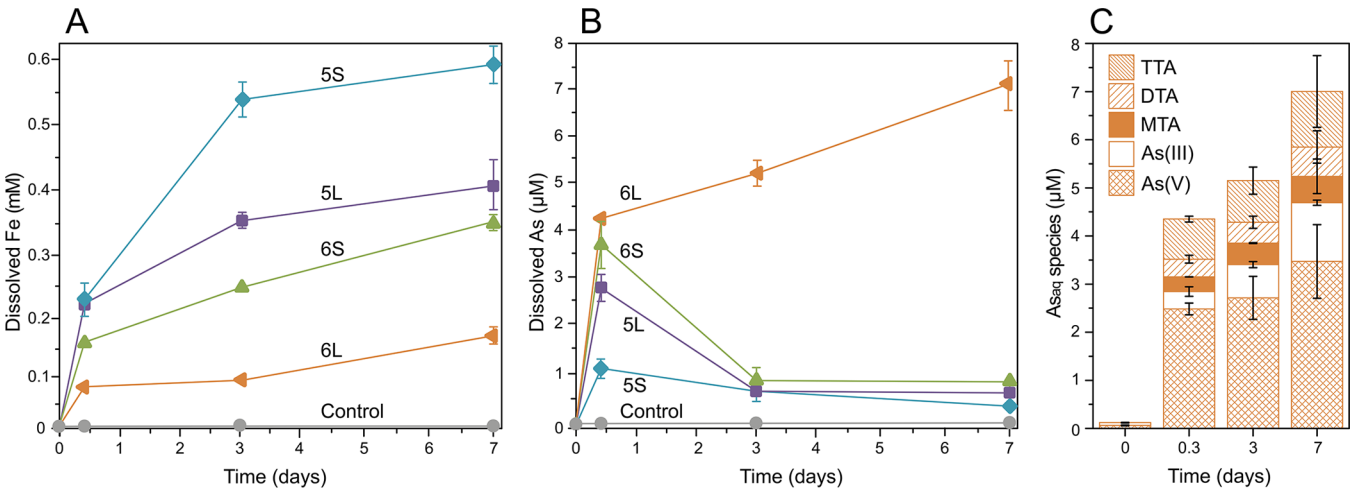

Figure 1. (A) Dissolved Fe, (B) total As_{aq}, and (C) aqueous As speciation for sample 6L $(S(-II)_{spike}/Fe = 1.62$; As_{aq} species recovery: 74−107%) determined in 0.22-μm filtrates. Error bars indicate the standard deviation calculated from triplicate experiments. Abbreviations: As(V): arsenate excluding thioarsenates, As(III): arsenite, MTA: monothioarsenate, DTA: dithioarsenate, TTA: trithioarsenate. Aqueous As speciation data of additional samples can be found in Table S12.

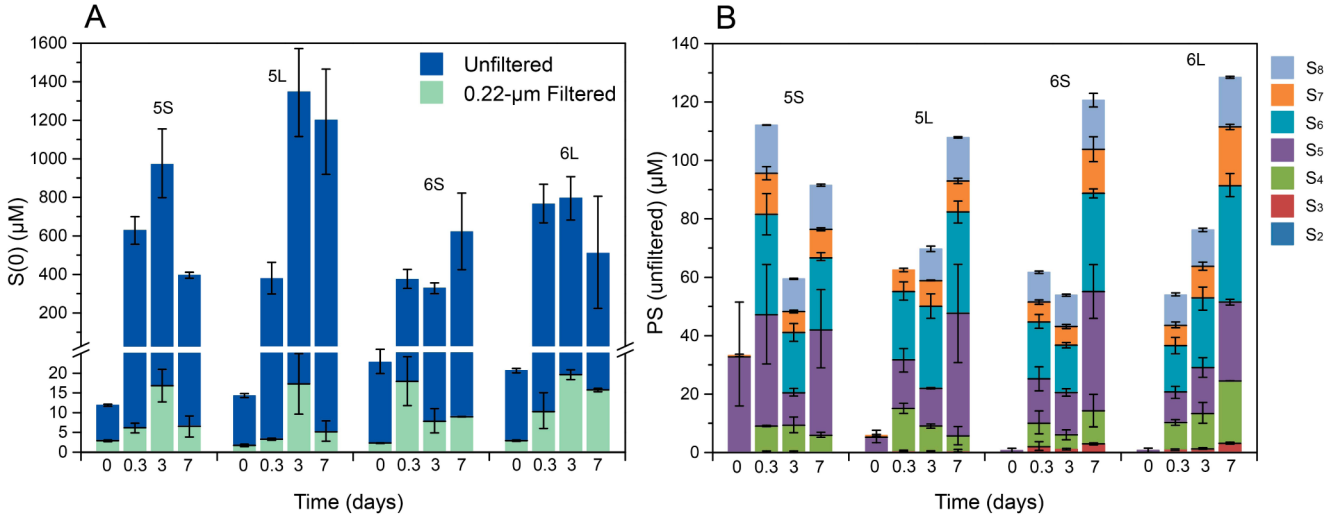

Figure 2. (A) Elemental S (S(0)) determined in unfiltered and 0.22-μm filtered samples and (B) polysulfides (PS) determined in unfiltered samples. Polysulfide concentrations in 0.22-μm filtrates were $\leq$ 5.1 μM (Figure S3). Error bars indicate the standard deviation calculated from triplicate experiments.

interferences cannot be excluded. Trends in dissolved sulfide were accompanied by a rapid decrease in E_h, which, on average, dropped from 377 ± 30 mV at the start of the experiment to −13 ± 53 mV at day 7 ($\pm\sigma$, n = 4; Table S7). Dissolved Fe concentrations (Fe_{aq}), assumed to be Fe(II), increased in all samples to 0.15−0.59 mM at day 7 (Figure 1A). In agreement with these trends, the solid-phase Fe concentrations decreased by 7.5−42.3 g/kg (Table S6). Dissolved Fe in the controls was low (<0.01 mM) and changed minimally within 7 days, indicating little biotic Fe reduction and negligible contributions of Fe-OM complexes to Fe_{aq} (Figure 1A). Total Fe_{aq} at day 7 was inversely related to the $S(-II)_{spike}/Fe$ molar ratios. For example, the lowest Fe_{aq} in sample 6L (0.15 mM) was associated with the highest $S(-II)_{spike}/Fe$ molar ratio (1.62) (cp. Figure 1A and Table S7). This inverse relation between Fe_{aq} and S(-II) has also been reported for natural porewater profiles of a minerotrophic fen,[34,35] and suggests the oxidation of sulfide by Fe(III)-(oxyhydr)oxides and subsequent precipitation of FeS (eq 3).

Sulfur Speciation: Wet Chemistry. Wet chemical S speciation analysis included determination of sulfate and thiosulfate in 0.22-μm filtered samples and S(0) and polysulfides in both 0.22-μm filtered and unfiltered samples. Low sulfate concentrations (19−48 μM) were detected in all samples and increased only slightly after sulfide addition (Table S8). Thiosulfate concentrations also increased after sulfide addition, averaging 305 ± 30 μM ($\pm\sigma$, n = 4) at 0.3 days. Thereafter, thiosulfate concentrations remained stable for the duration of the experiment (Table S8). Presuming our experiment ensured anoxic and abiotic conditions, thiosulfate may have formed through the oxidation of sulfide by Fe(III)-(oxyhydr)oxides[42] and/or by quinones[43] in floc OM. In agreement with earlier studies on sulfide reaction with Fe(III)-(oxyhydr)oxides,[11−13] S(0) was the dominant S oxidation product determined in sulfide-reacted flocs. In unfiltered samples, S(0) concentrations ranged between 390 and 1200 μM at 7 days, while <16 μM S(0) was determined in filtered samples (Figure 2A). Noteworthy, S(0) was already

DOI: 10.1021/acs.est.5b05791
Environ. Sci. Technol. 2016, 50, 3607−3616

detected at day 0 (<20 μM), suggesting that the flocs experienced partial reduction prior to sampling or processing. Our results generally show that S(0) was primarily associated with the solid-phase (Figure 2A). S(0) equilibrates with dissolved sulfide[40] and/or $Fe(II)_{surface}$,[13] leading to the formation of polysulfides

$$(n-1)S(0) + HS^- \leftrightarrow S_n^{2-} + H^+ \quad (4)$$

$$2Fe(II)_{surface} + S(0)_n + 2H_2O \leftrightarrow FeOOH + S_n^{2-} + 4H^+ \quad (5)$$

The overall reaction stoichiometry for polysulfide formation via sulfide-induced reduction of Fe(III)-oxyhydroxide has recently been recast by Wan et al.[44]

$$3nH_2S + 2nFeOOH \rightarrow (2n-1)FeS + Fe(II)_{surface} + S_{m+1}{}^{2-}{}_{surface} + [(n-m)/8]S_8 + 4nH_2O \quad (6)$$

where $S_{m+1}{}^{2-}{}_{surface}$ denotes surface polysulfides, n is the number of generated S(0) atoms, and m ($0 \le m \le n$) is the number of S(0) atoms associated with surface polysulfides. Eq 6 accounts for the fact that sulfide addition to goethite and lepidocrocite at neutral pH leads to the predominant formation (>99%) of surface-bound polysulfides.[44] Consistent with this, polysulfide concentrations in unfiltered floc samples far exceeded those in the filtered samples: 92−128 μM polysulfides were detected in unfiltered samples after 7 days, whereas filtered samples generally contained <1 μM polysulfides (Figures 2B and S3). The only exception was sample 6L in which dissolved polysulfide concentrations increased up to 5.1 μM after 3 days (Figure S3). Surface-bound polysulfides comprised mainly S_4^{2-}-S_8^{2-} species, with S_5^{2-} and S_6^{2-} accounting for the majority (49−68%) of all surface-bound polysulfides (Figure 2B), in accordance with the dominant polysulfide species expected at pH 7.[45,46]

Sulfur Speciation: X-ray Absorption Spectroscopy. Selected S K-edge X-ray absorption near edge structure (XANES) spectra of floc samples are shown in Figure 3, and results from the deconvolution of all spectra are presented in Tables S9 and S10. For additional spectra, see Figure S4. All floc samples were characterized by three distinct peak ranges. The first, relating to "reduced" S species (~2470−2475 eV), includes inorganic sulfides, organic exocyclic and heterocyclic S, and elemental S. It should be noted that the small difference between white-line energies of organic exocyclic and elemental S (<1 eV) renders the differentiation between these reduced S species impossible. The second peak range (~2475−2479 eV) hosts sulfoxide and sulfone S as "intermediate oxidized" S species, whereas the third peak range (~2479−2485 eV) accommodates "oxidized" S species and includes sulfonate and sulfate S. Despite differences in initial floc S/C/Fe molar ratios (Tables S6 and S7), S speciation in unreacted flocs was similar and dominated by reduced S species, with inorganic sulfide, exocyclic/elemental, and heterocyclic S comprising 17−29%, 32−44%, and 17−22% of total S, respectively. Contributions from oxidized and intermediate oxidized S species were minor (<10%) (Figures 3 and S4; Tables S9 and S10). Despite that small peaks for intermediate oxidized S species could be fitted, their abundance was likely overestimated due to postedge absorption features of reduced S species.

Immediately after sulfide addition, solution colors changed from brown to black, indicating the formation of Fe sulfides.[13,44] Solid-phase S contents increased by 125 ± 21 g/kg. This increase was slightly more pronounced for the small floc fractions, likely due to their higher Fe contents (Table S6). Sulfur XANES spectra of sulfide-reacted flocs showed an intensification in the peak assigned to inorganic sulfide S (~2470 eV) (Figure 3). Accordingly, inorganic sulfide S comprised 87 ± 2% of total S in all samples at 7 days (Table S10). Attempts to fit two Gaussians with white-line energies corresponding to intermediate oxidized S species failed, implying that sulfoxide and sulfone S contributions were low

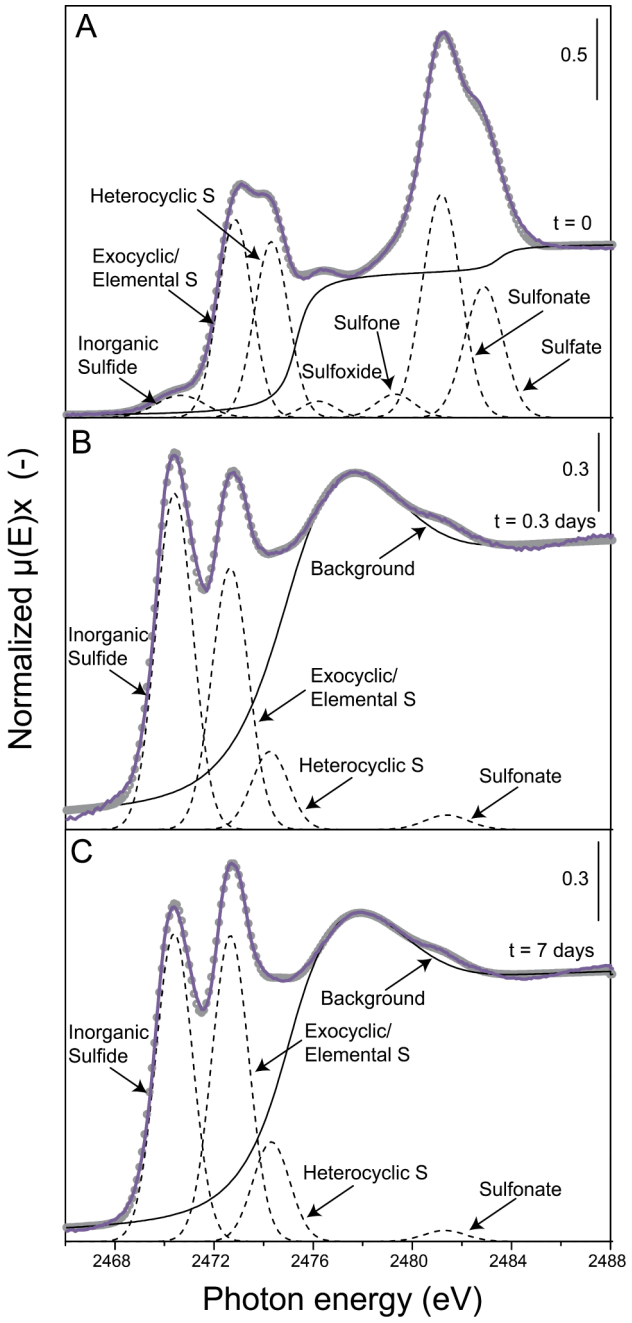

Figure 3. Deconvolution of normalized bulk S K-edge XANES spectra of sample 5L. The spectra of unreacted flocs (A) were decomposed into 7 Gaussians and 2 arctangent functions, whereas sulfide-reacted floc samples (B−C) required 4 Gaussians and 1 arctangent function. The broad peak feature at 2475−2479 eV in sulfide-reacted flocs is a postedge absorption feature of inorganic sulfide S[53] and thus was included in the background. Additional S K-edge XANES spectra and their results are presented in SI section 7.

DOI: 10.1021/acs.est.5b05791
Environ. Sci. Technol. 2016, 50, 3607−3616

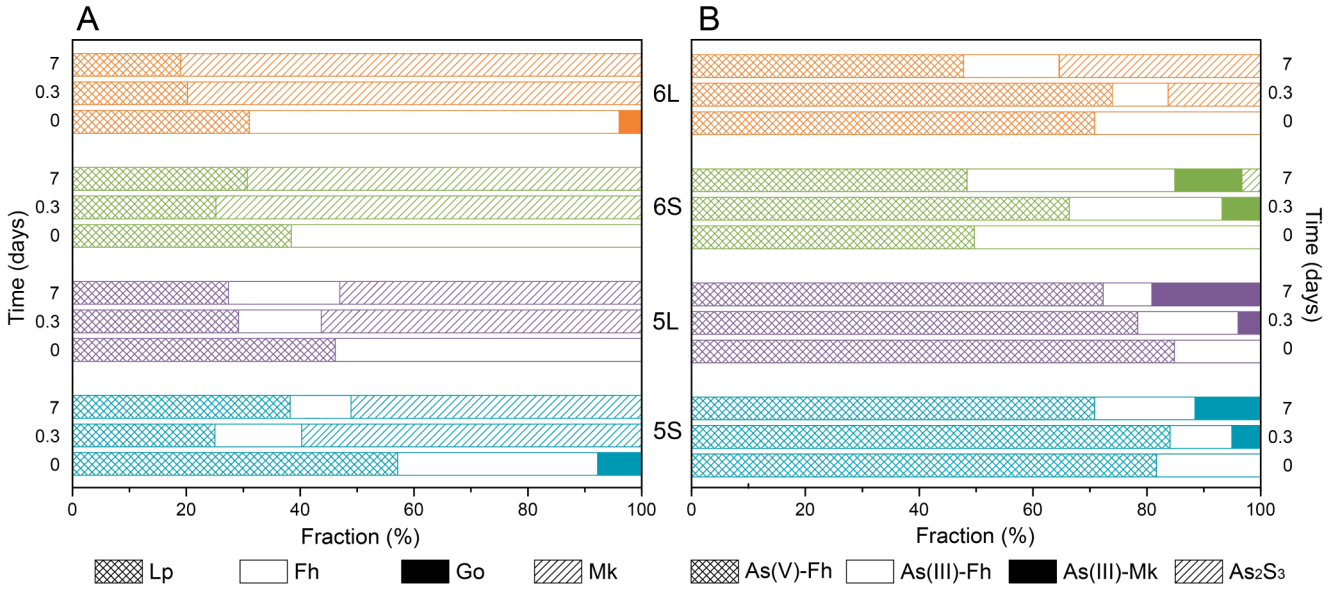

Figure 4. Linear combination fit (LCF) results of (A) bulk Fe K-edge EXAFS spectra and (B) bulk As K-edge EXAFS spectra. The horizontal bars display the percent fraction of each reference compound fitted in the LCF analysis. The bulk speciation results are presented in Tables S11 (Fe) and S13 (As). Abbreviations: Lp = lepidocrocite, Fh = ferrihydrite, Go = goethite, Mk = mackinawite, As(V)-Fh = arsenate-adsorbed ferrihydrite, As(III)-Fh = arsenite-adsorbed ferrihydrite, As(III)-Mk = arsenite-adsorbed mackinawite, As_2S_3 = orpiment-like As sulfide. Note that As reference spectra for arsenate-adsorbed ferrihydrite and arsenate-adsorbed mackinawite are almost indistinguishable (Figure S9).

and that the broad peak at 2475−2479 eV in sulfide-reacted flocs was background.[47,48] Though exocyclic/elemental S accounted for only 9−12% of total S in sulfide-reacted flocs at 7 days, when considering the floc S contents, these species showed individual increases of 12.3 ± 3.1 g/kg. These values are less than the increases in solid-phase associated S(0) determined by wet chemistry at 7 days (24.8 ± 12.8 g/kg), indicating a systematic underestimation of exocyclic/elemental S in the S XANES analysis.[48,49] Heterocyclic S in sulfide-reacted flocs increased by 1.8 ± 0.6 g/kg, which suggests the formation of aryl polysulfides.[43] A small Gaussian peak at ∼2481 eV additionally indicated that sulfonate was the only detectable oxidized S species, contributing ≤0.2% to total S in sulfide-reacted flocs.

Iron Speciation: Bulk X-ray Absorption Spectroscopy. Normalized Fe K-edge XANES spectra of unreacted flocs exhibited first-derivative maxima at ∼7128 eV, implying the predominance of Fe(III) (Figure S5). After sulfide addition, the XANES maxima shifted to ∼7119 eV, in agreement with the formation of Fe(II) (Figure S5). Changes in the bulk Fe speciation were evaluated by linear combination fitting (LCF) of k^3-weighted Fe K-edge extended X-ray absorption fine structure (EXAFS) spectra. Iron reference compounds were selected based on principal component analysis and target-transform testing (PCA-TT) (Tables S2 and S3). The LCF results are summarized in Figure 4A and Table S11, and the spectra and their fits are shown in Figure S6. Unreacted flocs contained 35−65% ferrihydrite ($\bar{x}$ = 54%) and 30−57% lepidocrocite, with a slightly higher lepidocrocite content noted for small compared to large flocs. Small quantities (≤8%) of goethite were also detected in some unreacted floc samples (Figure 4A). After reaction with sulfide for 7 days, all samples contained 52−81% mackinawite ($\bar{x}$ = 64%). These values agree well with mackinawite contents calculated from the inorganic sulfide fractions obtained by S XANES analysis (2.95 ± 0.47 mol mackinawite-Fe vs 3.48 ± 0.61 mol inorganic sulfide-S). The mackinawite formed was poorly crystalline as revealed by a weak and broad XRD peak at d = 1.81 Å corresponding to the 112 reflection of mackinawite (Figure S7).[50] The LCF analyses also showed a preferential decline in the floc ferrihydrite content, while lepidocrocite still accounted for 19−38% of total Fe at 7 days (Figure 4A). This result suggests a preferential reduction of ferrihydrite over lepidocrocite, despite the X-ray amorphous nature of floc lepidocrocite[3] (Figure S7). Assuming that the sulfide-induced reduction of nanocrystalline floc lepidocrocite and ferrihydrite proceeded similarly fast, our findings may alternatively suggest the neoformation of lepidocrocite after reaction of ferrihydrite with $Fe(II)_{aq}$ (0.15−0.59 mM, Figure 1A). This interpretation is in line with the rapid ferrihydrite-lepidocrocite conversion (5×10^{-3} mmol Fe/s) observed in low-Fe(II) (0.2 mM) and sulfate-free solutions at pH 7.2.[14]

Arsenic Speciation: Wet Chemistry. Mobilization of As was observed in all samples, with dissolved As concentrations (As_{aq}) far exceeding the drinking water limit of ∼0.13 μM (10 μg/L) recommended by the World Health Organization.[51] In samples 5S, 5L, and 6S As_{aq} reached maxima of 1.2−3.8 μM at 0.3 days and declined to 0.45−0.96 μM at 7 days. Only sample 6L showed continual increases in As_{aq}, eventually reaching 7.0 μM at 7 days (Figure 1B). The solution concentrations of As at day 7 accounted for 2.6−73% of total As (Tables S6, S12, and S14). Because As_{aq} in the controls remained low (<0.15 μM), initial increases in As_{aq} (<0.3 days) must be ascribed to the sulfide-triggered release of arsenite and arsenate from floc Fe(III)-(oxyhydr)oxides.[3] The subsequent drop in As_{aq} in three out of four samples implies readsorption of As onto mackinawite, (neoformed) Fe(III)-(oxyhydr)oxides, and/or the formation of As sulfides. Arsenic speciation measurements in the 0.22-μm filtrates yielded mediocre As recoveries (18−131%) in all but the 6L samples (74−107%, Table S12), which may be caused by Fe precipitation and subsequent As sorption during analysis. Nonetheless, this data shows that arsenate prevailed in all solutions, followed by arsenite and thioarsenates. The formation of mono-, di-, and

DOI: 10.1021/acs.est.5b05791
Environ. Sci. Technol. 2016, 50, 3607−3616

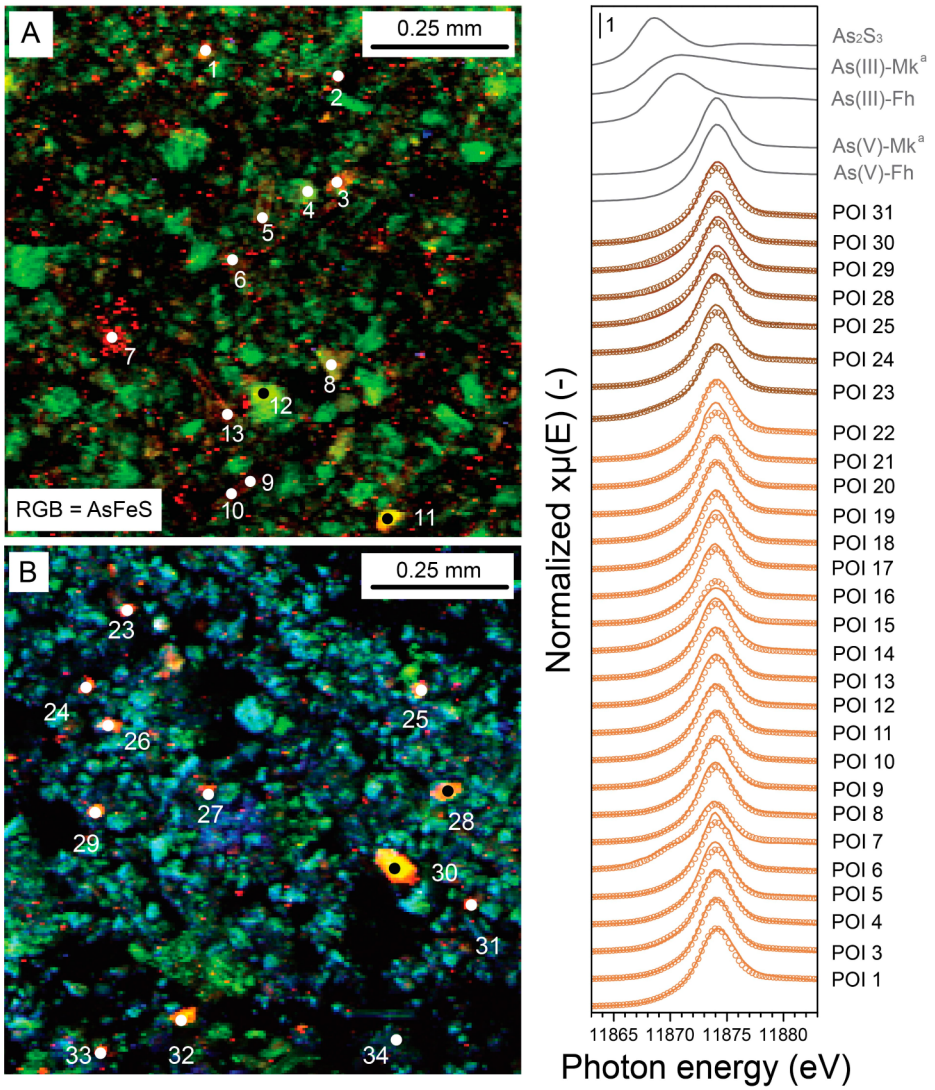

Figure 5. Tricolor μ-XRF maps of (A) unreacted and (B) sulfide-reacted (day 7) flocs of sample 6L showing the distributions of As (red), Fe (green), and S (blue). Maps were collected at 13.7 keV (As and Fe) and 6.9 keV (S) in continuous scan mode. Numbered points of interest (POI) indicate spots selected for μ-XANES analyses. Right: Linear combination fits (LCF) of As K-edge μ-XANES spectra from unreacted (POIs 1-22) and sulfide-reacted flocs (POIs 23-25, 28-31). Experimental data and LCFs are shown in solid and dotted lines, respectively. Reference spectra employed in the LCF analysis are shown in gray. The fits were performed over an energy range of −20−30 eV ($E-E_0$) with no constraints (initial fit sums: 100 ± 1%). The initial fit fractions were recalculated to 100% and are reported in Table S15. Iron K-edge μ-XANES spectra as well as an additional μ-XRF map can be found in the SI. [a]Spectrum from ref 21.

trithioarsenate was evident in all sulfide-reacted samples, indicating that arsenite released from floc Fe(III)-(oxyhydr)-oxides was partially oxidized by S(0)[23,24] or sulfide.[25] In sample 6L, thiolated As species contributed up to 33% of As_{aq} (Figure 1C and Table S12). The formation of thioarsenates in conjunction with the lowest residual Fe(III) mineral content, which caused a loss of sorption sites particularly for the dominant As species arsenate, therefore provides a plausible explanation for continuous As release in sample 6L (Figures 1B and 4A).

Arsenic Speciation: Bulk X-ray Absorption Spectroscopy. Normalized As K-edge XANES spectra of unreacted flocs exhibited two first-derivative maxima at ∼11870 and ∼11874 eV, implying the presence of both As(III) and As(V) (Figure S8). After sulfide addition, the ∼11870 eV maxima became generally more pronounced indicating an increased fraction of As(III). Only in sample 6L did the ∼11870 eV maximum shift toward lower energy values (∼11869 eV) typical of As sulfide minerals (Figure S8). Changes in the bulk As speciation were evaluated by LCF of k^3-weighted As K-edge EXAFS spectra (Figure S9), and the results are summarized in Figure 4B and Table S13. In agreement with our earlier findings,[3] spectra of unreacted flocs were well fit by a combination of Fe(III)-associated arsenate (50−85%, $\bar{x}$ = 72%) and arsenite. Fit references considered for sulfide-reacted flocs were determined after PCA-TT analyses (Tables S4 and S5). Because the spectra for arsenate-adsorbed ferrihydrite and mackinawite are nearly identical (Figure S9), only arsenate-adsorbed ferrihydrite was used in the final data analysis for Fe-associated arsenate. The obtained LCF results show that Fe-associated arsenate in sulfide-reacted flocs decreased up to 23% ($\bar{x}$ = 13%) at 7 days (Figure 4B, Table S13). The fraction of arsenite-adsorbed Fe(III)-(oxyhydr)oxides changed little in the site 5 samples and decreased by at most 15% in site 6 samples (Figure 4B, Table S13). At the end of the experiment, arsenite-adsorbed Fe sulfide (11−19%) was present in all samples

DOI: 10.1021/acs.est.5b05791
Environ. Sci. Technol. 2016, 50, 3607−3616

except for sample 6L, which instead comprised 35% As sulfide (Figure 4B, Table S13). The latter result suggests As_2S_3 formation during coprecipitation of arsenate and mackinawite.[21] Interestingly, the floc arsenite content increased at lower $S(-II)_{spike}$/Fe molar ratios (0.75 and 0.92; samples 5S and 5L, respectively) by ~12% at 7 days (Table S13), indicating the presence of surface-associated S-species and excess Fe(II) in these samples may have facilitated arsenate reduction, as adsorbed arsenate is not reduced at the mackinawite surface in the absence of sulfide.[21,52] In summary, our bulk speciation analyses showed that solid-phase As was still largely associated with Fe after floc sulfidization and that As sulfide formation was only encountered at the highest $S(-II)_{spike}$/Fe molar ratios (1.00 and 1.62; samples 6S and 6L, respectively). Because arsenate-adsorbed ferrihydrite and mackinawite are difficult to distinguish by As XAS, we additionally employed As and Fe μ-XAS to identify the primary Fe sorbent for arsenate after sulfide addition (next section).

Elemental Distributions and Local Arsenic and Iron Speciation. To investigate the microscale distribution and speciation of As, Fe, and S in flocs, sample 6L was analyzed by μ-XRF spectrometry and μ-XANES spectroscopy. Figures 5 and S10 depict μ-XRF maps illustrating the distributions of As, Fe, and S before and after sulfide addition. The elemental maps of the unreacted flocs (Figures 5A and S10) indicated the association of As with Fe and showed evidence of As hotspots coinciding with the presence of green algae *Closterium* spp.[3] Sulfur hotspots were limited and likely associated with OM. Contrastingly, in sulfide-reacted 6L flocs, Fe and S showed similar spatial distributions throughout the sample, whereas As enrichments were limited to Fe-rich and S-poor points (Figure 5B). These As-rich points of interest (POIs) were selected for further As and Fe K-edge μ-XANES spectroscopy analysis. Selected As μ-XANES spectra of the POIs are shown in the right panel of Figure 5, along with their LCFs whose results are summarized in Table S15. The spectral analysis showed that As in hotspots of both unreacted and sulfide-reacted flocs was primarily present in its pentavalent oxidation state (68−95 and 78−87%, respectively). The corresponding Fe μ-XANES spectra of the sulfide-reacted 6L flocs exhibited prepeak centroid positions (7113 ± 1 eV) consistent with Fe(III) (Figure S11), documenting little to no Fe reduction in the As-rich POIs despite abundant mackinawite formation (Figure 4A). This result implies that arsenate preferentially adsorbed to residual or neoformed Fe(III)-(oxyhydr)oxides. Thus, for sample 6L, the near complete reduction of Fe(III)-(oxyhydr)-oxides to mackinawite at 7 days (81% of total Fe_{solid}) likely contributed to the enhanced As release (Figure 1B). Arsenic K-edge μ-XANES spectra also revealed that arsenite adsorbed to mackinawite accounted for up to 14% of total As in sample 6L, and only one spectrum (POI 23) showed evidence of As_2S_3 formation (Table S15).

ENVIRONMENTAL IMPLICATIONS

Our previous study showed that Fe-rich organic freshwater flocs have a high capacity for trace metal(loid) sorption, effectively acting as an As sink under oxic conditions.[3] In contrast, this study documents an enhanced mobilization of floc-associated As in pH-neutral sulfidic solutions, despite the abundant precipitation of Fe and As sulfides and the presence of residual Fe(III)-(oxyhydr)oxides. Arsenic solution trends appear to be mainly controlled by the readsorption of arsenate released upon floc sulfidization to residual (or neoformed) Fe(III)-(oxyhydr)oxides rather than precipitated Fe sulfides. Floc sulfidization triggers the rapid formation (<0.3 days) of solid-phase associated S(0) and polysulfides; both key reactants involved in pyrite formation. This could explain the occurrence of pyrite, arsenian pyrite ($FeAs_nS_{2-n}$), and arsenopyrite (FeAsS) in *Gola di Lago* peat.[10,29] The excessive formation of surface-bound S(0) likely fosters the rapid conversion of floc arsenite into thioarsenates, species possessing lower sorption tendencies than As oxyanions and hence an increased mobility.[26,27] Our results indicate that thioarsenates can be expected to be common porewater constituents in the As-enriched *Gola di Lago* peatland and show that As-rich organic freshwater flocs may become a source of aqueous As under sulfate-reducing conditions. Thus our findings highlight the importance of seasonal redox cycles in S-rich wetland systems for the fate of floc-associated trace metal(loid)s.

ASSOCIATED CONTENT

Supporting Information

The Supporting Information is available free of charge on the ACS Publications website at DOI: 10.1021/acs.est.5b05791.

Details on floc sampling, XAS data collection, reduction, and analyses, total element contents of flocs, experimental conditions, aqueous and solid-phase speciation as well as additional element distribution data (PDF)

AUTHOR INFORMATION

Corresponding Author

*Phone: 45-35334364. E-mail: mikutta@plen.ku.dk.

Notes

The authors declare no competing financial interest.

ACKNOWLEDGMENTS

We are grateful to K. Barmettler, M. Simmler, J. Scharper (ETH Zurich), and S. Will (Bayreuth University) for assisting with sample preparation and analysis. We acknowledge SSRL and APS, both User Facilities of the U.S. Department of Energy Office of Science operated by Stanford University, contract No. DE-AC02-76SF00515 (SSRL) and Argonne National Laboratory, contract No. DE-AC02-06CH11357 (APS) for the provision of synchrotron radiation facilities. We thank R. Davis and E. Nelson (SSRL) and A. Lanzirotti and M. Newville (APS) for their support during the synchrotron measurements. This project was funded by the SNSF (Project 200021_127157).

REFERENCES

(1) Elliott, A. V. C.; Plach, J. M.; Droppo, I. G.; Warren, L. A. Comparative floc-bed sediment trace element partitioning across variably contaminated aquatic ecosystems. *Environ. Sci. Technol.* **2012**, *46*, 209−216.

(2) Plach, J. M.; Elliott, A. V. C.; Droppo, I. G.; Warren, L. A. Physical and ecological controls on freshwater floc trace metal dynamics. *Environ. Sci. Technol.* **2011**, *45*, 2157−2164.

(3) ThomasArrigo, L. K.; Mikutta, C.; Byrne, J.; Barmettler, K.; Kappler, A.; Kretzschmar, R. Iron and arsenic speciation and distribution in organic flocs from streambeds of an arsenic-enriched peatland. *Environ. Sci. Technol.* **2014**, *48*, 13218−13228.

(4) Droppo, I. G. Rethinking what constitutes suspended sediment. *Hydrol. Processes* **2001**, *15*, 1551−1564.

(5) Droppo, I. G.; Leppard, G. G.; Flannigan, D. T.; Liss, S. N. The freshwater floc: A functional relationship of water and organic and

DOI: 10.1021/acs.est.5b05791
Environ. Sci. Technol. 2016, 50, 3607−3616

inorganic floc constituents affecting suspended sediment properties. *Water, Air, Soil Pollut.* **1997**, *99*, 43−53.
(6) Larsen, L. G.; Harvey, J. W.; Crimaldi, J. P. Morphologic and transport properties of natural organic floc. *Water Resour. Res.* **2009**, *45*, W01410.
(7) Larsen, L. G.; Harvey, J. W.; Noe, G. B.; Crimaldi, J. P. Predicting organic floc transport dynamics in shallow aquatic ecosystems: Insights from the field, the laboratory, and numerical modeling. *Water Resour. Res.* **2009**, *45*, W01411.
(8) Elliott, A. V. C.; Warren, L. A. Microbial engineering of floc Fe and trace metal geochemistry in a circumneutral, remote lake. *Environ. Sci. Technol.* **2014**, *48*, 6578−6587.
(9) González, A. Z. I.; Krachler, M.; Cheburkin, A. K.; Shotyk, W. Spatial distribution of natural enrichments of arsenic, selenium, and uranium in a minerotrophic peatland, Gola di Lago, Canton Ticino, Switzerland. *Environ. Sci. Technol.* **2006**, *40*, 6568−6574.
(10) Langner, P.; Mikutta, C.; Kretzschmar, R. Arsenic sequestration by organic sulphur in peat. *Nat. Geosci.* **2012**, *5*, 66−73.
(11) Poulton, S. W.; Krom, M. D.; Raiswell, R. A revised scheme for the reactivity of iron (oxyhydr)oxide minerals towards dissolved sulfide. *Geochim. Cosmochim. Acta* **2004**, *68*, 3703−3715.
(12) Poulton, S. W. Sulfide oxidation and iron dissolution kinetics during the reaction of dissolved sulfide with ferrihydrite. *Chem. Geol.* **2003**, *202*, 79−94.
(13) Hellige, K.; Pollok, K.; Larese-Casanova, P.; Behrends, T.; Peiffer, S. Pathways of ferrous iron mineral formation upon sulfidation of lepidocrocite surfaces. *Geochim. Cosmochim. Acta* **2012**, *81*, 69−81.
(14) Hansel, C. M.; Benner, S. G.; Fendorf, S. Competing Fe(II)-induced mineralization pathways of ferrihydrite. *Environ. Sci. Technol.* **2005**, *39*, 7147−7153.
(15) Kocar, B. D.; Borch, T.; Fendorf, S. Arsenic repartitioning during biogenic sulfidization and transformation of ferrihydrite. *Geochim. Cosmochim. Acta* **2010**, *74*, 980−994.
(16) Pedersen, H. D.; Postma, D.; Jakobsen, R.; Larsen, O. Fast transformation of iron oxyhydroxides by the catalytic action of aqueous Fe(II). *Geochim. Cosmochim. Acta* **2005**, *69*, 3967−3977.
(17) Saalfield, S. L.; Bostick, B. C. Changes in iron, sulfur, and arsenic speciation associated with bacterial sulfate reduction in ferrihydrite-rich systems. *Environ. Sci. Technol.* **2009**, *43*, 8787−8793.
(18) Burton, E. D.; Johnston, S. G.; Bush, R. T. Microbial sulfidogenesis in ferrihydrite-rich environments: Effects on iron mineralogy and arsenic mobility. *Geochim. Cosmochim. Acta* **2011**, *75*, 3072−3087.
(19) Burton, E. D.; Johnston, S. G.; Planer-Friedrich, B. Coupling of arsenic mobility to sulfur transformations during microbial sulfate reduction in the presence and absence of humic acid. *Chem. Geol.* **2013**, *343*, 12−24.
(20) Cummings, D. E.; Caccavo, F.; Fendorf, S.; Rosenzweig, R. F. Arsenic mobilization by the dissimilatory Fe(III)-reducing bacterium *Shewanella alga* BrY. *Environ. Sci. Technol.* **1999**, *33*, 723−729.
(21) Farquhar, M. L.; Charnock, J. M.; Livens, F. R.; Vaughan, D. J. Mechanisms of arsenic uptake from aqueous solution by interaction with goethite, lepidocrocite, mackinawite, and pyrite: An X-ray absorption spectroscopy study. *Environ. Sci. Technol.* **2002**, *36*, 1757−1762.
(22) Wang, Y.; Morin, G.; Ona-Nguema, G.; Juillot, F.; Guyot, F.; Calas, G.; Brown, G. E. Evidence for different surface speciation of arsenite and arsenate on green rust: An EXAFS and XANES study. *Environ. Sci. Technol.* **2010**, *44*, 109−115.
(23) Couture, R.-M.; Van Cappellen, P. Reassessing the role of sulfur geochemistry on arsenic speciation in reducing environments. *J. Hazard. Mater.* **2011**, *189*, 647−652.
(24) Stauder, S.; Raue, B.; Sacher, F. Thioarsenates in sulfidic waters. *Environ. Sci. Technol.* **2005**, *39*, 5933−5939.
(25) Planer-Friedrich, B.; Haertig, C.; Lohmayer, R.; Suess, E.; McCann, S. H.; Oremland, R. Anaerobic chemolithotrophic growth of the haloalkaliphilic bacterium strain MLMS-1 by disproportionation of monothioarsenate. *Environ. Sci. Technol.* **2015**, *49*, 6554−6563.
(26) Couture, R.-M.; Rose, J.; Kumar, N.; Mitchell, K.; Wallschläger, D.; Van Cappellen, P. Sorption of arsenite, arsenate, and thioarsenates to iron oxides and iron sulfides: A kinetic and spectroscopic investigation. *Environ. Sci. Technol.* **2013**, *47*, 5652−5659.
(27) Suess, E.; Planer-Friedrich, B. Thioarsenate formation upon dissolution of orpiment and arsenopyrite. *Chemosphere* **2012**, *89*, 1390−1398.
(28) O'Day, P. A.; Vlassopoulos, D.; Root, R.; Rivera, N. The influence of sulfur and iron on dissolved arsenic concentrations in the shallow subsurface under changing redox conditions. *Proc. Natl. Acad. Sci. U. S. A.* **2004**, *101*, 13703−13708.
(29) Langner, P.; Mikutta, C.; Suess, E.; Marcus, M. A.; Kretzschmar, R. Spatial distribution and speciation of arsenic in peat studied with microfocused X-ray fluorescence spectrometry and X-ray absorption spectroscopy. *Environ. Sci. Technol.* **2013**, *47*, 9706−9714.
(30) Hoffmann, M.; Mikutta, C.; Kretzschmar, R. Bisulfide reaction with natural organic matter enhances arsenite sorption: Insights from X-ray absorption spectroscopy. *Environ. Sci. Technol.* **2012**, *46*, 11788−11797.
(31) Bottrell, S. H.; Hatfield, D.; Bartlett, R.; Spence, M. J.; Bartle, K. D.; Mortimer, R. J. G. Concentrations, sulfur isotopic compositions and origin of organosulfur compounds in pore waters of a highly polluted raised peatland. *Org. Geochem.* **2010**, *41*, 55−62.
(32) Boulegue, J.; Lord, C. J.; Church, T. M. Sulfur speciation and associated trace-metals (Fe, Cu) in the pore waters of Great Marsh, Deleware. *Geochim. Cosmochim. Acta* **1982**, *46*, 453−464.
(33) Luther, G. W.; Church, T. M.; Scudlark, J. R.; Cosman, M. Inorganic and organic sulfur cycling in salt-marsh pore waters. *Science* **1986**, *232*, 746−749.
(34) Koretsky, C. M.; Haas, J. R.; Ndenga, N. T.; Miller, D. Seasonal variations in vertical redox stratification and potential influence on trace metal speciation in minerotrophic peat sediments. *Water, Air, Soil Pollut.* **2006**, *173*, 373−403.
(35) Koretsky, C. M.; Haveman, M.; Beuving, L.; Cuellar, A.; Shattuck, T.; Wagner, M. Spatial variation of redox and trace metal geochemistry in a minerotrophic fen. *Biogeochemistry* **2007**, *86*, 33−62.
(36) Planer-Friedrich, B.; London, J.; McCleskey, R. B.; Nordstrom, D. K.; Wallschläger, D. Thioarsenates in geothermal waters of yellowstone national park: Determination, preservation, and geochemical importance. *Environ. Sci. Technol.* **2007**, *41*, 5245−5251.
(37) Cline, J. D. Spectrophotometric determination of hydrogen sulfide in natural waters. *Limnol. Oceanogr.* **1969**, *14*, 454−458.
(38) Kamyshny, A.; Ekeltchik, I.; Gun, J.; Lev, O. Method for the determination of inorganic polysulfide distribution in aquatic systems. *Anal. Chem.* **2006**, *78*, 2631−2639.
(39) Rizkov, D.; Lev, O.; Gun, J.; Anisimov, B.; Kuselman, I. Development of in-house reference materials for determination of inorganic polysulfides in water. *Accredit. Qual. Assur.* **2004**, *9*, 399−403.
(40) Kamyshny, A.; Borkenstein, C. G.; Ferdelman, T. G. Protocol for quantitative detection of elemental sulfur and polysulfide zero-valent sulfur distribution in natural aquatic samples. *Geostand. Geoanal. Res.* **2009**, *33*, 415−435.
(41) Siegel, L. M. A direct microdetermination for sulfide. *Anal. Biochem.* **1965**, *11*, 126−132.
(42) Pyzik, A. J.; Sommer, S. E. Sedimentary iron monosulfides: Kinetics and mechanism of formation. *Geochim. Cosmochim. Acta* **1981**, *45*, 687−698.
(43) Heitmann, T.; Blodau, C. Oxidation and incorporation of hydrogen sulfide by dissolved organic matter. *Chem. Geol.* **2006**, *235*, 12−20.
(44) Wan, M.; Shchukarev, A.; Lohmayer, R.; Planer-Friedrich, B.; Peiffer, S. Occurrence of surface polysulfides during the interaction between ferric (hydr)oxides and aqueous sulfide. *Environ. Sci. Technol.* **2014**, *48*, 5076−5084.
(45) Giggenbach, W. Optical spectra and equilibrium distribution of polysulfide ions in aqueous solution at 20°. *Inorg. Chem.* **1972**, *11*, 1201−1207.

DOI: 10.1021/acs.est.5b05791
Environ. Sci. Technol. 2016, 50, 3607−3616

(46) Schwarzenbach, G.; Fischer, A. Die acidität der sulfane und die zusammensetzung wässeriger polysulfidlösungen. *Helv. Chim. Acta* **1960**, *43*, 1365−1390.
(47) Shakeri Yekta, S.; Gustavsson, J.; Svensson, B. H.; Skyllberg, U. Sulfur K-edge XANES and acid volatile sulfide analyses of changes in chemical speciation of S and Fe during sequential extraction of trace metals in anoxic sludge from biogas reactors. *Talanta* **2012**, *89*, 470−477.
(48) Manceau, A.; Nagy, K. L. Quantitative analysis of sulfur functional groups in natural organic matter by XANES spectroscopy. *Geochim. Cosmochim. Acta* **2012**, *99*, 206−223.
(49) Prietzel, J.; Botzaki, A.; Tyufekchieva, N.; Brettholle, M.; Thieme, J.; Klysubun, W. Sulfur speciation in soil by S K-edge XANES spectroscopy: Comparison of spectral deconvolution and linear combination fitting. *Environ. Sci. Technol.* **2011**, *45*, 2878−2886.
(50) Lennie, A. R.; Redfern, S. A. T.; Schofield, P. F.; Vaughan, D. J. Synthesis and Rietveld crystal structure refinement of mackinawite, tetragonal FeS. *Mineral. Mag.* **1995**, *59*, 677−683.
(51) WHO, *Guidelines for Drinking-Water Quality*; World Health Organization: Geneva, 2011; p 315−318.
(52) Wolthers, M.; Charlet, L.; Van der Weijden, C. H.; Van der Linde, P. R.; Rickard, D. Arsenic mobility in the ambient sulfidic environment: Sorption of arsenic(V) and arsenic(III) onto disordered mackinawite. *Geochim. Cosmochim. Acta* **2005**, *69*, 3483−3492.
(53) Burton, E. D.; Bush, R. T.; Sullivan, L. A.; Hocking, R. K.; Mitchell, D. R. G.; Johnston, S. G.; Fitzpatrick, R. W.; Raven, M.; McClure, S.; Jang, L. Y. Iron-monosulfide oxidation in natural sediments: Resolving microbially mediated S transformations using XANES, electron microscopy, and selective extractions. *Environ. Sci. Technol.* **2009**, *43*, 3128−3134.

DOI: 10.1021/acs.est.5b05791
Environ. Sci. Technol. 2016, 50, 3607−3616